M&C 2017 - International Conference on Mathematics & Computational Methods Applied to Nuclear Science & Engineering, Jeju, Korea, April 16-20, 2017, on USB (2017)

Validation of McCARD for VHTR core with HTTR Benchmark

Jinsu Park[a], Tae Yong Han[b], Hyun Chul Lee[c,*], Deokjung Lee[a]

[a]*Department of Nuclear Engineering, UNIST, UNIST-gil 50, Ulsan, 44919, Korea*
[b]*Korea Atomic Energy Research Institute, 111, Daedeok-daero 989beon-gil, Yuseong-gu, Daejeon, Korea*
[c]*Pusan National University, 2, Busandaehak-ro 63beon-gil, Geunjeong-gu, Busan 46241, Korea*
[*]*Corresponding author: hyunchul.lee@pusan.ac.kr*

Abstract – *In this paper, high temperature engineering test reactor (HTTR) benchmark were analyzed using McCARD and the ability to analyze a very high temperature gas-cooled reactor (VHTR) core of McCARD was validated. The specification of HTTR core is described and it is suggested that the approximation method of geometry for modelling in computational code. The multiplication factor during the fuel loading (HTTR-FC), the control rod insertion depth for critical condition (HTTR-CR), and isothermal temperature coefficient (HTTR-TC) are estimated by McCARD using both ENDF/B-VII.0 and ENDF/B-VII.1 neutron cross section libraries. The maximum difference of multiplication factor between result of McCARD and experiment data of HTTR-FC and HTTR-CR is around 600pcm by using ENDF/B-VII.1 library. Although the discrepancy of isothermal temperature coefficient (ITC) from McCARD is different with the experiment data, it is similar with estimated ITC from Japan and France.*

I. INTRODUCTION

High temperature engineering test reactor (HTTR) is constructed by Japan atomic energy research institute (JAERI) and it is graphited-moderated and helium gas-cooled reactor with an outlet temperature of 950°C and a power of 30MW_{th}. The HTTR is suitable for a benchmark problem because the geometry of reactor core is complex and experiment data can be accessed [1]. In many countries, a reactor analysis codes for very high temperature gas-cooled reactor have been validated by comparing a numerical result of computer code and experiment data from HTTR benchmark [2, 3].

McCARD is a Monte Carlo neutron transport code developed for the neutronics analysis of various nuclear system [4]. The code can handle a complex geometry using composition cells which can be used again through translation. Also, the randomly distributed fuel particle in high temperature gas-cooled reactor can be explicitly treated.

Section 2 describes the HTTR benchmark specification. Section 3 demonstrates the method of modelling in McCARD including approximation of geometry. Section 4 presents the numerical results of McCARD by comparing the experiment data from HTTR benchmark.

II. DESCRIPTION OF HTTR BENCHMARK

The HTTR was developed to improve a technological basis of advanced high temperature gas-cooled reactors (HTRGs) and to conduct a various irradiation experiment. It achieved a first criticality through annular shape fuel loading. The HTTR benchmark provides a various experiment data. The behavior of multiplication factor during fuel loading for first criticality (HTTR-FC), the control rod insertion depth for critical condition (HTTR-CR), and the isothermal temperature coefficient (HTTR-TC) are provided as experiment data and those data is used in this research. Also, the HTTR benchmark provides a detail specification of core geometry and the material of fuel, reflector, and control rod.

1. Fuel Assembly

The fuel assembly used in the HTTR core includes 33 or 31 fuel rods and 2 burnable poison rods in the hexagonal graphite block. The fuel rod is composed of graphite sleeve and 14 fuel compact which has coated fuel particles. Fig. 1 shows the configuration of the fuel rod.

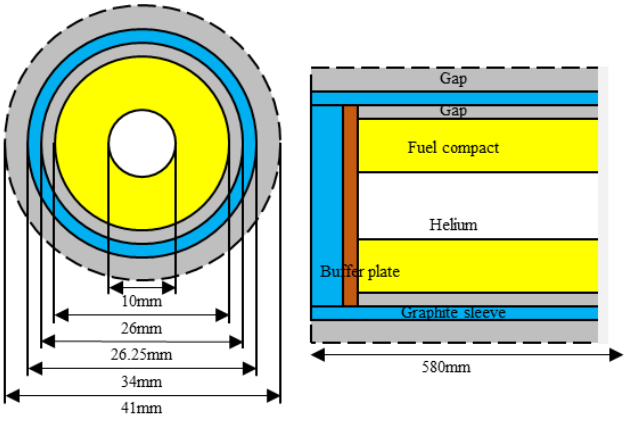

Fig. 1. Configuration of fuel rod.

A. Fuel Compact and Coated Fuel Particle

The fuel rod includes 14 fuel compacts, which is composed of coated fuel particle in the annular cylinder graphite matrix. There are 12 types of coated fuel particle with various enrichment of ^{235}U. The coated fuel particle

consists of sphere shape low enriched UO_2 kernel with a Tristructural-isotropic (TRISO) coating. Also, the TRISO coating consists of a low density, porous pyrolytic carbon (PyC) buffer layer adjacent to the fuel kernel, followed by high density isotropic PyC layer, a SiC layer and, a final outer PyC layer. Table I presents the detail specification of 12 types of the coated fuel particle used in HTTR. The configuration of fuel compact and coated fuel particle is shown in Fig. 2.

Table I. Specification of various coated fuel particle

	Type	A01	A02	A03	A04
Fuel kernel	Enrichment (wt.%)	3.301	3.864	4.290	4.794
	Density (g/cm^3)	10.80	10.75	10.78	10.76
	Outer diameter (μm)	609.0	594.4	593.6	594.9
	Impurity (ppm)	0.92	0.89	0.92	0.94
1st layer	Density (g/cm^3)	1.158	1.091	1.112	1.110
	Thickness (μm)	59.1	61.7	61.3	60.9
2nd layer	Density (g/cm^3)	1.873	1.879	1.905	1.907
	Thickness (μm)	30.9	30.4	30.5	30.3
3rd layer	Density (g/cm^3)	3.206	3.207	3.206	3.205
	Thickness (μm)	29.8	28.9	29.2	29.1
4th layer	Density (g/cm^3)	1.855	1.858	1.869	1.905
	Thickness (μm)	46.4	45.7	46.2	45.2
	Type	A05	A06	A07	A08
Fuel kernel	Enrichment (wt.%)	5.162	5.914	6.254	6.681
	Density (g/cm^3)	10.76	10.77	10.74	10.73
	Outer diameter (μm)	591.8	592.4	593.5	593.2
	Impurity (ppm)	1.24	0.96	1.13	0.95
1st layer	Density (g/cm^3)	1.118	1.112	1.122	1.121
	Thickness (μm)	60.4	60.3	60.4	60.8
2nd layer	Density (g/cm^3)	1.893	1.909	1.909	1.902
	Thickness (μm)	30.7	30.8	31.1	31.0
3rd layer	Density (g/cm^3)	3.205	3.204	3.205	3.208
	Thickness (μm)	29.4	29.3	28.7	28.7
4th layer	Density (g/cm^3)	1.846	1.890	1.870	1.860
	Thickness (μm)	45.7	45.9	45.0	46.1
	Type	A09	A10	A11	A12
Fuel kernel	Enrichment (wt.%)	7.189	9.820	9.358	9.810
	Density (g/cm^3)	10.77	10.82	10.79	10.81
	Outer diameter (μm)	594.0	608.1	593.1	591.4
	Impurity (ppm)	0.90	0.92	0.88	0.88
1st layer	Density (g/cm^3)	1.147	1.143	1.170	1.152
	Thickness (μm)	64.9	58.7	61.1	59.3
2nd layer	Density (g/cm^3)	1.894	1.878	1.902	1.879
	Thickness (μm)	31.0	29.2	31.9	30.5
3rd layer	Density (g/cm^3)	3.202	3.201	3.207	3.202
	Thickness (μm)	28.6	28.7	28.2	26.7
4th layer	Density (g/cm^3)	1.867	1.869	1.848	1.853
	Thickness (μm)	46.2	45.6	46.0	46.3

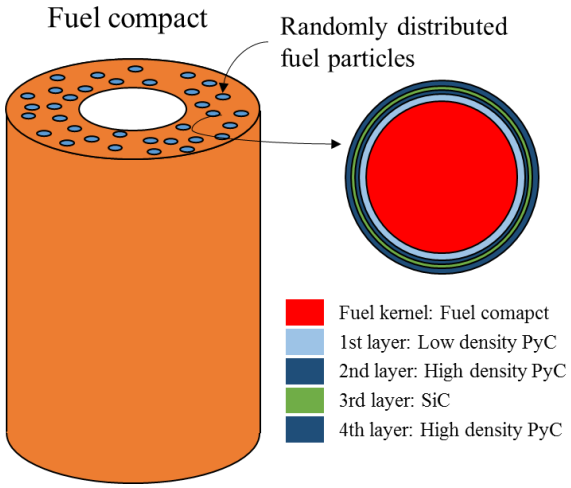

Fig. 2. Configuration of fuel compact and coated fuel particle.

B. Burnable Poison Rod

The fuel assembly has 3 holes for insertion of burnable poison rod and 2 burnable poison rods are inserted. The burnable poison rod is composed of a 20 B_4C pellets (40cm) and 20 graphite disks (10cm). There are two types of burnable poison rod, H-1 type use 2.22wt.% and H-2 type use 2.74wt.% enrichment of ^{10}B. Fig. 3 shows the cross section of fuel assembly including 33 fuel holes.

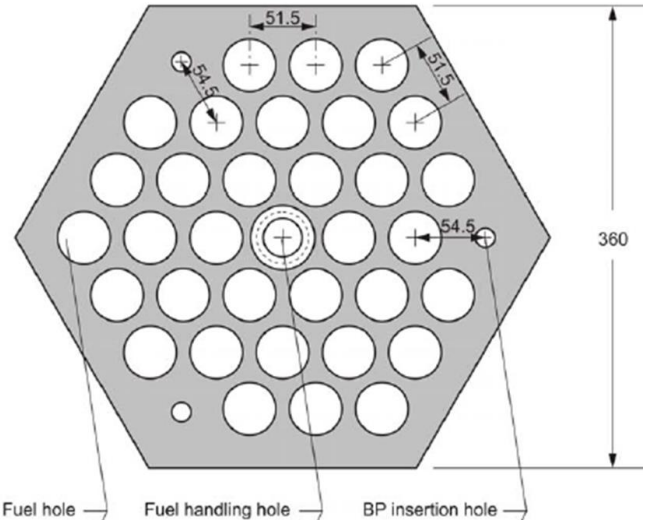

Fig. 3. Configuration of fuel assembly (33 fuel holes).

2. Control Rod Guide Block, Replaceable Reflector Block, and Dummy Fuel Block

Except fuel block, there are control rod guide block, replaceable reflector block in the HTTR core. The control

rod guide block has 2 holes for control rod insertion and 1 hole for insertion of reserved shutdown system (RSS) at accident situation. There are 12 replaceable reflector blocks in the active core and top and bottom of the core. The reflector block located at the top and bottom of the core has 2.3cm diameter holes for coolant flow and the lowest reflector block has 6 large holes. The dummy fuel block is inserted in the core before fuel loading and it will be substituted with the fuel block one by one during fuel loading.

3. Permanent Reflector Block

The HTTR core components are surrounded by 12 polygonal shape permanent reflector block. There are several holes for the irradiation experiment and the void fraction of permanent reflector block with hole is 0.7%.

III. MCCARD MODELLING

The 3-dimensional HTTR core is modelled using McCARD. The Monte Carlo calculations are performed with ENDF-B/VII.0 and ENDF/B-VII.1 continuous energy neutron cross section libraries. The simulation parameters are 200,000 histories per cycle, 100 inactive cycles, and 400 active cycles to set a standard deviation of the multiplication factor under 20pcm.

The fuel compact with randomly distributed coated fuel particles is explicitly modelled in McCARD using FCEL card. Because the coated fuel particle cells cannot be overlapped and cut by surface, it can be occurred that the sensitivity along the height of fuel compact cell. Therefore, the height of fuel compact was set to exactly same with real height of fuel compact in the HTTR benchmark.

1. Approximation of Geometry

Several parts of geometries are approximated in modelling because of the limitation of McCARD and the simplicity for modelling. The cone shape cannot be modelled in McCARD, the chopped cone shape structures are approximated to cylinder shape structures with volume weighting. All blocks have chopped cone shape fuel handling hole for the insertion and withdrawal of block during fuel loading. Fig. 4 shows approximation of fuel handling hole model.

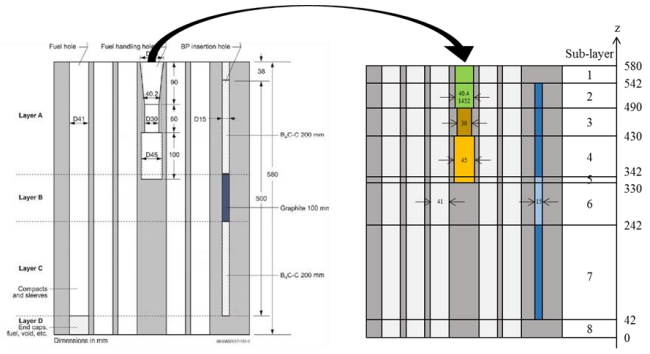

Fig. 4. Approximation of the fuel handling hole model.

Except the fuel handling hole, the holes for insertion of control rod and RSS in the control rod guide block are chopped cone shape. Fig. 5 and 6 show the approximation of control rod insertion hole in 6th layer and RSS insertion hole in 7th layer of control rod guide block.

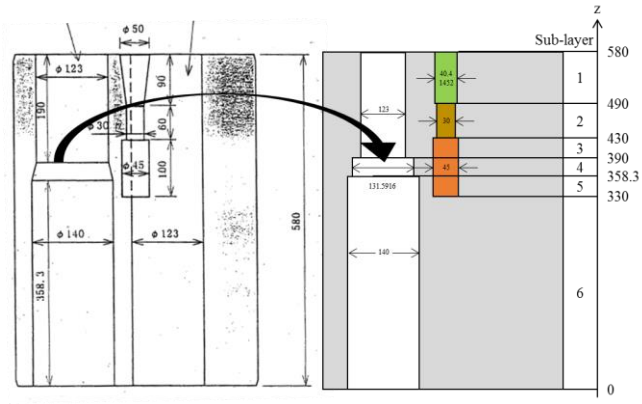

Fig. 5. Approximation of the control rod insertion hole in control rod guide block at 6th layer.

Fig. 6. Approximation of the RSS insertion hole in control rod guide block at 7th layer.

The coolant channel, which existed in replaceable reflector block at lowest region of core, is approximated to hexagon with volume weighting due to simplicity of modelling. Fig. 7 shows approximation of the coolant channel in replaceable reflector block at 9th layer.

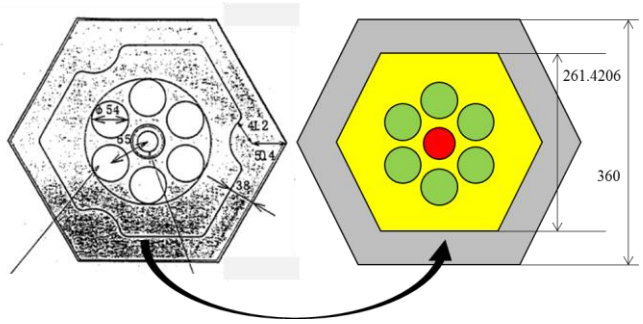

Fig. 7. Approximation of the coolant channel in replaceable reflector block at 9th layer.

The dodecagonal shape permanent reflector block is approximated to cylinder shape with volume weighting of graphite. Also, several holes in the block for irradiation experiment is ignored in McCARD model. Therefore, the number density of permanent reflector block is modified by considering the void fraction.

IV. NUMERICAL RESULTS

In this section, the numerical results of McCARD are presented. Among various experiment data in HTTR benchmark, HTTR-FC, HTTR-CR, and HTTR-TC data are produced by McCARD.

1. HTTR-FC

The Monte Carlo simulation is performed step by step through substituting the pre-inserted dummy fuel block with the fuel block. Fig. 8 shows the fuel loading order of HTTR-FC.

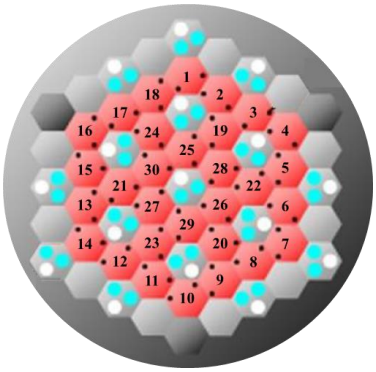

Fig. 8. Fuel loading order of HTTR-FC.

The McCARD calculations are performed with ENDF/B-VII.0 and ENDF/B-VII.1 neutron cross section library. Table II represents the effective multiplication factors and the difference with experiment data. The difference of multiplication factor between McCARD and experiment data decrease when ENDF-B/VII.1 library used. From the result of HTTR-FC, the discrepancy of McCARD with experiment data is around 600pcm. Fig. 9 shows the behavior of multiplication factor during fuel loading.

Table II. Multiplication factors of HTTR-FC

Fuel Columns	Experiment k_{eff}	McCARD (ENDF-B/VII.0)		
		k_{eff}	SD (pcm)	Diff. (pcm)
9	0.92820	0.94575	16	1755
12	0.94810	0.96926	14	2116
15	0.96520	0.98620	16	2100
16	0.97010	0.99154	15	2144
17	0.97850	1.00117	15	2267
18	0.99130	1.01345	16	2215
19	1.01520	1.03210	14	1690
21	1.04170	1.06148	15	1978
24	1.08340	1.10191	15	1851
27	1.11980	1.13344	15	1364
30	1.13460	1.14040	15	580
Fuel Columns	**Experiment k_{eff}**	**McCARD (ENDF-B/VII.1)**		
		k_{eff}	SD (pcm)	Diff. (pcm)
9	0.92820	0.93129	14	309
12	0.94810	0.95434	15	624
15	0.96520	0.97108	15	588
16	0.97010	0.97617	14	607
17	0.97850	0.98506	14	656
18	0.99130	0.99768	14	638
19	1.01520	1.01686	14	166
21	1.04170	1.04704	14	534
24	1.08340	1.08885	14	545
27	1.11980	1.12194	14	214
30	1.13460	1.13004	14	-456

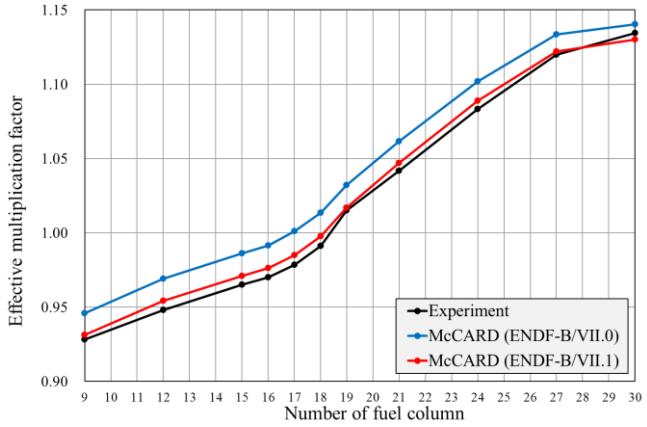

Fig. 9. Behavior of multiplication factor during fuel loading.

The major difference of the ENDF/B-VII.0 and ENDF/B-VII.1 libraries for analysis of VHTR core is capture cross section of carbon. Generally, the material of moderator used in the VHTR is graphite, the change of cross section of graphite can occur significant reactivity change. Fig. 10 shows capture cross section of carbon in the ENDF/B-VII.0 and ENDF/B-VII.1 library. In 0.01 to 2MeV energy ration, capture cross section of ENDF/B-VII.1 is larger than that of ENDF/B-VII.0. The larger cross section of ENDF/B-VII.1 decreases the multiplication factor and the results can be accurate.

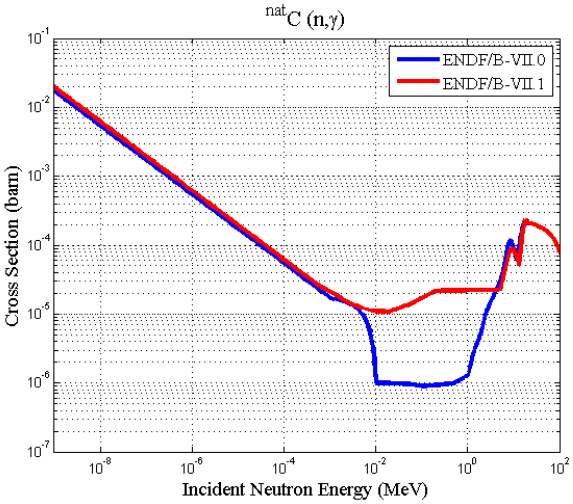

Fig. 10. Behavior of multiplication factor during fuel loading.

2. HTTR-CR

The HTTR benchmark provides the control rod insertion depth from 19 to 30 fuel columns core. There are 4 bunches of control rod; C, R1, R2, and R3. Table III presents the information of control rod sets.

Table III. Information of control rod sets

Type	Location of control rod
C	A01
R1	C01, C03, C05, C07, C09, C11
R2	E03, E07, E11, E15, E19, E23
R3	E01, E09, E17

There are three types of control rod behavior pattern. First pattern is flat standard (FS) pattern, the control rods named C, R1, and R2 are inserted in same level and R3 rods are fully withdrawn. Second pattern is F23 pattern, the R2 and R3 rods located in core periphery region are inserted in same level and C and R1 rods are fully withdrawn. Last pattern is C pattern, only C rods are inserted and other rods are fully withdrawn. Table IV represents the measured control rod insertion depth for critical condition.

Table IV. Measured control rod depth for critical conditions.

Case	Fuel Columns	Critical rod position (mm)				Remark
		C	R1	R2	R3	
1	19	1739	4050	3325	4050	C
2	21	2647	2645	2646	4049	FS
3	24	2213	2215	2215	4049	FS
4	24	4051	4050	1593	1592	F23
5	27	1901	1899	1899	4050	FS
6	30	1775	1775	1775	4049	FS

The Monte Carlo simulation of each fuel columns core with various control rod location are performed with both ENDF/B-VII.0 and ENDF/B-VII.1. Table V represents the multiplication factors of HTTR-CR. As shown in the result of HTTR-FC, the difference of multiplication factor between McCARD and experiment data decrease when ENDF/B-VII.1 library used. The effect of difference of library is gradually reduced with the fuel loading. Along the fuel loading, the amount of fuel in the core is increased and it leads to reduction of effect of graphite.

Table V. Multiplication factors of HTTR-CR.

Case	Experiment k_{eff}	McCARD (ENDF-B/VII.0)		
		k_{eff}	SD (pcm)	Diff. (pcm)
1	1.00049	1.01575	16	1526
2	1.00037	1.02001	15	1964
3	1.00037	1.01566	15	1529
4	1.00037	1.01276	15	1239
5	1.00037	1.00931	25	894
6	1.00025	1.00650	15	625
Case	**Experiment k_{eff}**	**McCARD (ENDF-B/VII.1)**		
		k_{eff}	SD (pcm)	Diff. (pcm)
1	1.00049	1.00311	14	262
2	1.00037	1.00620	14	583
3	1.00037	1.00396	15	359
4	1.00037	1.00216	14	179
5	1.00037	0.99895	15	-142
6	1.00025	0.99783	15	-242

3. HTTR-TC

The isothermal temperature coefficients (ITC) are calculated from the difference of multiplication factor for the 30 fuel columns core. Although the control rod insertion depth should be changed due to thermal expansion of control rod along the increment of core temperature, the control rod insertion depth is fixed to obtain the difference of multiplication factor. The McCARD simulations are performed for 300K, 400K, 500K, and 600K as a core temperature with both ENDF/B-VII.0 and ENDF/B-VII.1

libraries. The isothermal temperature coefficient of the fully-loaded core can be evaluated from the effective multiplication factors, using following relationship.

$$\rho_n = \frac{k_{n+1} - k_n}{k_{n+1} \cdot k_n} \cdot \frac{1}{T_{n+1} - T_n}. \quad (1)$$

The ρ_n is the temperature coefficient between T_n and T_{n+1}, the T_n is the core temperature n^{th} simulation, the T_{n+1} is the core temperature $(n+1)^{th}$ simulation, k_n is the effective multiplication factor at T_n, and k_{n+1} is the effective multiplication factor at T_{n+1}. Table VI represents a multiplication factors and ITC of HTTR-TC.

There is 2~3pcm/K difference of ITC between the ITC calculated by McCARD and the experiment data. Also, the effect of different library is not reflected in the ITC calculation.

Table VI. Multiplication factors and ITC of HTTR-TC.

Temperature (K)	**Experiment (%dk/k/K *10^{-4})**	**McCARD (ENDF-B/VII.0)**		
		***k*eff**	**SD (pcm)**	**ITC**
300	From -1.4 to -1.3	1.00650	15	-1.599
400		0.99056	13	-1.588
500		0.97522	14	-1.578
600		0.96044	14	-
Temperature (K)	**Experiment (%dk/k/K *10^{-4})**	**McCARD (ENDF-B/VII.1)**		
		***k*eff**	**SD (pcm)**	**ITC**
300	From -1.4 to -1.3	0.99783	15	-1.595
400		0.98220	15	-1.573
500		0.96726	14	-1.543
600		0.95304	14	-

V. CONCLUSIONS

In this paper, the accuracy of McCARD for analyzing VHTR core is demonstrated by using the HTTR benchmark problems. The geometry and material specifications of HTTR benchmark problem are described and modelling methods of complex geometry of HTTR system are also presented. Among HTTR benchmark problem sets, the HTTR-FC, HTTR-CR, and HTTR-TC situations are simulated by McCARD using both ENDF/B-VII.0 and ENDF/B-VII.1 neutron cross section libraries. When the ENDF-B/VII.1 library used, the differences of multiplication factor between McCARD and experiment data are around 200~600pcm. The change of capture cross section of carbon in ENDF/B-VII.1 library is major reason of the accuracy improvement of VHTR core analysis. The ability of McCARD for analyzing VHTR core is validated through this research, it is expected that McCARD can be utilized for VHTR core design and analysis.

ACKNOWLEDGMENTS

REFERENCES

1. N. Nojiri, et el, “Benchmark Problems Data for the HTTR’s Start-up Core Physics Experiments,” JAERI-memo 10-005, Japan Atomic Energy Research Institute (1998).
2. J. D. Bess, et el, “Evaluation of the Start-up Core Physics Tests at Japan’s High Temperature Engineering Test Reactor (Fully-Loaded Core),” INL/EXT-08-14767, Idaho National Laboratory (2009).
3. A. Badulescu, et el, “Evaluation of High Temperature Gas Cooled Reactor Performance: Benchmark Analysis related to Initial Testing of the HTTR and HTR-10,” IAEA-TECDOC-1382, International Atomic Energy Agency (2003).
4. H. J. Shim, et el, “McCARD: Monte Carlo Code for Advanced Reactor Design and Analysis,” *Nuclear Engineering and Technology*, 44, 161-176 (2012).